Available online at **www.joac.info**

ISSN: 2278-1862

Journal of Applicable Chemistry

2020, 9 (5): 691-708

(International Peer Reviewed Journal)

Novel Method for Preparation of Nanoscale NaX zeolite from Vietnamese Rice husk and Kaolinite and its Application in Upgrading low Quality Diesel Fuel

Don N. Ta[1], Hong K. D. Nguyen[1]*, Quang V. Nguyen[2] and Duong V. Le[1]

1. HanoiUniversity of Scienceand Technology, DaiCoViet, Hanoi-10000, **VIETNAM**
2. Petroleum Technical Institute, HaNoi, **VIETNAM**

Email: dieuhongprof@gmail.com

Accepted on 15th August, 2020

ABSTRACT

This research covers studies on preparation of nanoscale NaX zeolite from Vietnamese rice husk and kaolinite as sources of silicon and aluminum. The prepared nanoscale zeolite named Nano-NaX is applied in the upgrading adsorption process of low quality diesel fuel. The materials are characterized by X-ray Diffraction (XRD), Scanning Electron Microscope (SEM) and Transmission Electron Microscopy (TEM). The as-prepared material has the crystallinity reached 95% and particle size reached 45 nm. The diesel samples were studied for the composition analysis and commercial criteria analysis. After treatment diesel fuel products fully meet the current commercial specifications of diesel fuel.

Graphical Abstract

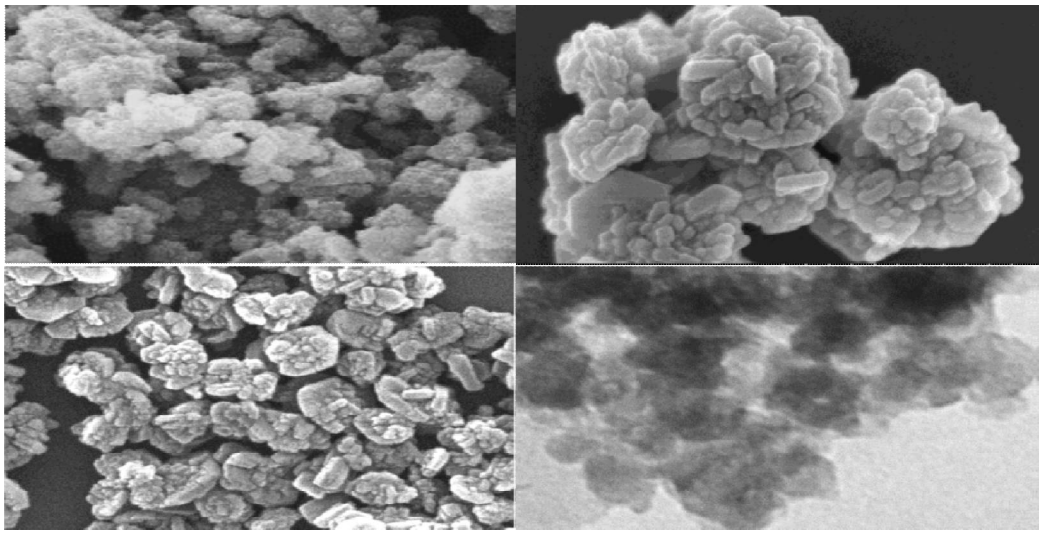

SEM and TEM images of the catalyst

Keywords: Nano NaX zeolite, Nanocrystals, Synthesis, Rce husk ash, Kaolinite.

INTRODUCTION

In recent years, in order to take advantage of natural raw materials and waste materials in agricultural production, the world has paid more attention on using kaolin as a source to supply aluminum and rice husk ash to supply silicon for synthesizing a number of different zeolites. There have been published works synthesizing zeolites from kaolin such as synthesis of zeolite NaX [**1**], NaAzeolite [**1, 2**], zeoliteNaY [**3**], zeolite N [**4**], zeolite ZSM-5 [**5, 6**], zeolite Beta [**7**]. Some works fabricating zeolites from rice husk ash such as synthesizing NaAzeolite [**8, 11**], zeolite NaX [**9, 12, 13**], zeoliteNaY [**10, 14**], zeolite ZSM-5 [**15**], zeolite ZSM- 11 [**16**]. When synthesized from kaolin, the silicon component is mainly in the form of clean chemicals such as sodium silicate. When synthesized from rice husk ash, the aluminum component is usually sodium aluminate or aluminum sulfate. There have been not many published researches of zeolites synthesis which use kaolinite and rice husk ash simultaneously without any further silicon or aluminum sources. Until now, there have been a few studies are reported [**17**] presenting the results of low quality mixture of zeolite P and analcim synthesis, report [**18**] synthesized meso-zeolite and report [**19**] published the synthesis of MSU-S(Y). Recently, research [**20**] brought out the synthesis of zeolite Y, zeolite P from kaolinite and quartz, research [**21**] applied rice husk ash and kaolinite in the fabrication of zeolite mordenite. Take Nano NaX zeolite into consideration, recently, there have been a number of researches published the synthesis from clean chemicals [**22, 23**], from kaolinite [**24**], yet, there have been not any reports published that used simultaneously kaolinite and rice husk ash to synthesis nano-NaX successfully. Obviously, the simultaneous use of both sources of kaolin and rice husk ash to synthesize porous materials in general and micro-porous materials in particular needs further research and this paper presents the very first results of the synthesis of Nano-NaX from rice husk ash and kaolin in the conditions of hydrothermal crystallization under normal conditions, without using organic structural agents.

Low quality diesel fuel is the fuel generated during the operation of a ship when there is direct contact between fuel and seawater, the indicators of commercial quality analysis are not qualified. To treat the low quality diesel fuel, nano NaX zeolite synthesized from rice husk and kaolin was used to adsorb agents deteriorating fuel to improve commercial indicators and diesel fuel after treatment is reusable. This research presents systematically the results of synthesis of nano NaX zeolite and investigation of the effects of a number of factors that affect the synthesis in hydrothermal crystallization in normal condition with any further organic structural agents and its application in low quality diesel fuel treatment.

MATERIALS AND METHODS

Materials: Raw rice husk was washed many times with water to remove insoluble impurities, dried at 80°C, then treated with 5% HCl acid with the ratio of husk to acid equal to 1/5 (g mL^{-1}) at room temperature for 6 h, then washed off Cl^- and dried at 100°C. Obtained rice husk after dried was calcined at 700°C for 4 h to collect ash containing mainly SiO_2 in amorphous form. Kaolin, after being exploited from the quarry, was filtered and washed off sand as well as gravel and dried. Then the material was treated with 4N hydrochloric acid at the ratio of solid to liquid equal to 2/3 (g m^{-1}) for 6 hours at 90°C, then filtered and washed off totally Cl- ion and dried at 100°C. Finally, the obtained material was heated for 3 hours at 650°C to form the sample called meta-caolanh.

Investigation of effects of factors on the synthesis of Nano-NaX: The rice husk ash was mixed with meta-caolanh, sodium hydroxide, sodium chloride and distilled water with molar ratio (3,5-5,0)$Na_2O.Al_2O_3$.(2-5)SiO_2.(140-170)H_2O.(0-2)NaCl. The mixture was aged for 24-72 h at room temperature with stirring, hydrothermal crystallization at 75-95°C for 12-36 h without stirring. The product after crystallization was washed with distilled water until the wash water has pH level equal to 8, dried at a temperature of 100°C and then crushed and sifted through a 0.15 mm sieve.

Treatment of low quality diesel fuel: The low quality diesel fuel generated after use is black. The results of analyzing and testing the content of substances contained in that diesel showed that the resin and asphantene content increased sharply (Table 1), the commercial specifications of this fuel were almost unsatisfactory according to TCVN 5689.

Table 1. Hydrocarbon content, naphthalene content, resin content, asphalthen content of commercial diesel, low quality diesel fuel, and diesel after treatment

S.No.	Sample name	Aromatic hydrocarbon content, %wt	Naphthalene content, %wt	Resin content mg 100 mL^{-1}	Asphalt content, %wt
1	Commercial diesel	18.45	8.23	22	0.01
2	Low quality diesel fuel	33.89	6.17	909	0.75
3	Diesel after treatment	25.23	7.37	8	0

The effects of reaction time on the adsorption efficiency in the low quality diesel fuel treatment were investigated according to the following procedure. Firstly, as-prepare catalyst was added into the adsorption column which has a diameter of 6 cm, length of 50 cm and a filter paper in the bottom. The height of the catalyst layer in the column is 15 cm. Waste fuels was poured into the column, running through the layer of adsorbent and the clean fuel came out from the bottom.

To investigate the effects of the stirring process, different amounts of as-prepared material were added into a beaker containing 100 mL of contaminated fuel and stirred for several different intervals from 0.5 to 2.5 h at room temperature.

To examine the effects of compression process, nano NaX zeolite was added into a adsorption column with 6 cm diameter and 50 cm length and a layer of filter paper inside the bottom and a weight of 5 kg on the top. A volume of 1 litter of waste diesel was poured into and running through a height of 15 cm of adsorbent inside the column which was compressed by a piston. The clean diesel was collected at the bottom of the column.

The effects of temperature were researched by adding the adsorbent into adsorption column with 6 cm diameter, 50 cm length and a layer of filter paper inside the bottom till its height reached 15 cm. Then 1 litter of contaminated fuel was poured into the column and clean fuel came out from the bottom. The temperature was change from 20°C to 35°C.

A number of different adsorbents were taken into consideration of their efficiencies such as Nano NaX zeolite, meta-kaolinite and silica gel in the same conditions, that they were all added into the column with 6 cm diameter, 50 cm length and filter paper inside the bottom. The height of the adsorbents was all 15 cm. And the fuel outputs were all from the bottom. The output products were tested for the resin content.

Characterization: The cation exchange capacity of all the samples was examined by Barium method [25] in environment of pH 7. The water adsorption and toluene adsorption were determined in stationary state after all samples were dried for 6 h, at a pressure of 4 mm Hg, at 180°C. In order to verify crystal structures of as-prepared materials, all samples were characterized by XRD on D8 ADVÀNCE-Bruker. Their crystallinity was calculated according to [26]. The particle size was determined from the average width FWHM of the characteristic peak corresponding to different 2θ values according to Scherrer's formula described in [27]. SEM images were taken from JSM 5410 LV and TEM images were taken from JEM 1010.

RESULTS AND DISCUSSION

The synthesis of zeolite Nano-NaX

Effects of alkali content: The effects of alkali content or the ratio of Na_2O/Al_2O_3 in gel to the crystallization of Nano-NaX from rice husk ash and meta-kaolinite is shown in figure 1, figure 2 and table 2. From the XRD results in figure 1, it shows that, when the ratio of Na_2O/Al_2O_3 in the reaction gel system changed from 3.5 to 5.0 with the step of 0.5, characteristic peaks off zeolite NaX in XRD charts of all 4 samples were appeared at $2\theta \approx 6.20$ with strong intensity. In addition, in XRD diagrams, strong peak at $2\theta \approx 26.70$ was also appeared, characteristic for α- quartz overlapping with a peak of NaX zeolite around $2\theta \approx 26.70$ [29]. The samples all have a fairly flat baseline, proving that these samples mainly contain crystal phases.

However, when the ratio of Na_2O/Al_2O_3 in the gel increases gradually, the characteristic peak intensity of the crystal phases changes significantly. Accordingly, the characteristic peak of NaX zeolite has increased intensity and reached the maximum corresponding to the ratio of Na_2O/Al_2O_3=4.0, then decreased afterwards. The characteristic peak pin width is also the maximum at this sample. The above results confirm the maximum crystallinity and the smallest NaX zeolite particle size when the ratio Na_2O/Al_2O_3= 4.0. From the XRD method, the crystallinity of zeolite NaX is determined approximately 95%, using Scherrer's equation to identify the crystals of NaX zeolite with an average size of 45 nm (Table 2). Thus, the sample that has low ratio Na_2O/Al_2O_3 in gel (NX-3.5N-figure 1a) does not give a high crystallinity of zeolite NaX. Thus, the sample with a low ratio of Na_2O/Al_2O_3 in the gel (NX-3.5N-figure 1a) gives low NaX zeolite crystallinity (88%-Table 2), possibly because in the same experimental conditions, when the ratio of Na_2O/Al_2O_3 in the gel is low, it means that alkali concentration is low or there are not enough Na+ ions to balance with the necessary number of AlO_4- tetrahedra to form a complete crystal of NaX zeolite. When the ratio of Na_2O/Al_2O_3 = 4.5, a weak peak at $2\theta \approx 28,1o$ is observed, which is characteristic for zeolite NaP1 (P1) [29]. When the Na_2O/Al_2O_3 ratio continues to be increased (sample NX-5.0N-figure 1d), the characteristic peak of NaP1 zeolite appears with a stronger intensity and accompanied by the appearance of hydroxysodalite with a characteristic peak at $2\theta \approx 24, 4o$ [30]. NaX zeolite crystallinities in samples NX-4.5N and NX-5.0N were determined by 91% and 63%, respectively. The sample NX-5.0N also contains 13% crystal zeolite NaP1. Obviously, when the Na_2O/Al_2O_3 ratio in gel continues to be increased gradually greater than 4, the concentration of Na +/AlO4- is also ascending and it is not selective for NaX zeolite (with open structure, 6-sided dual ring). at the same time. it tends to form the dense structure of NaP1 zeolite (four-sided monolithic ring) and extremely dense structure of thermodynamically [28] stable hydroxysodalite [30].

SEM and TEM images of 4 samples are presented in figure 2, showing that, when the ratio of Na_2O/Al_2O_3 in gel is increased, the average particle size according to both methods is at minimum at sample NX-4.0N with zeolite NaX crystal clearly and uniformly formed, 70 nm and 45 nm respectively, which is consistent with the results determined by the XRD method. A small part of amorphous background existed in the other 3 samples is carefully observed. Particularly, there are 2 crystals close to zeolite NAX and NaP1 appeared in the NX-5.0N sample with the size of 120 nm and 700 nm (SEM), 100 nm and 364 nm (TEM). According to the results of CEC, water and toluene adsorption listed in table 2 show a very good match with the crystallinity and particle size. The largest CEC of NX-4.0N sample is 320 meqBa_2^+/100 g (equivalent to 640 meqNH_4^+/100 g), which proves that this sample contains a lot of AlO_4- tetrahedra - and the ratio of Na_2O/Al_2O_3 = 4.0 in gel is the appropriate ratio to the maximum binding of Na + ions in the gel with the AlO_4- tetrahedra, giving the highest crystallinity (95 %) for this sample. That CEC is twice as high as CEC = 317 meqNH_4^+/100g when synthesizing NaX zeolite from rice husk ash and sodium aluminate [9]. On the other hand, the ratio of Na_2O/Al_2O_3 = 4.0 in this study is the lowest compared to the process of synthesizing NaX zeolite from different sources: equal to 5.5 [24] and 10, 9 [23] from clean chemicals, equal to 6.2 [22] from rice husk ash.

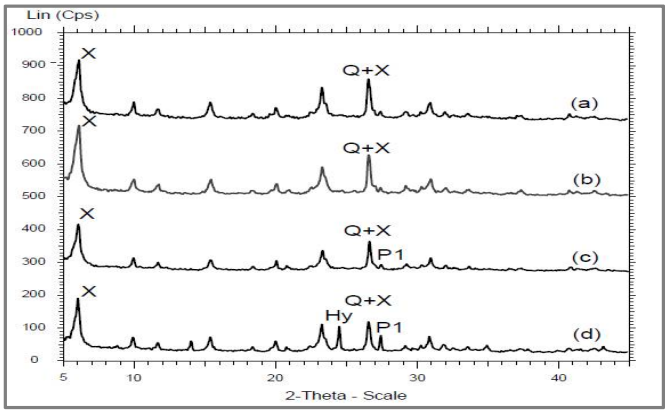

Figure 1. XRD diagram of the effects of alkali content on the crystallization of Nano-NaX: NX-3.5N (a), NX-4.0N (b), NX-4.5N (c) and NX-5.0N (d).

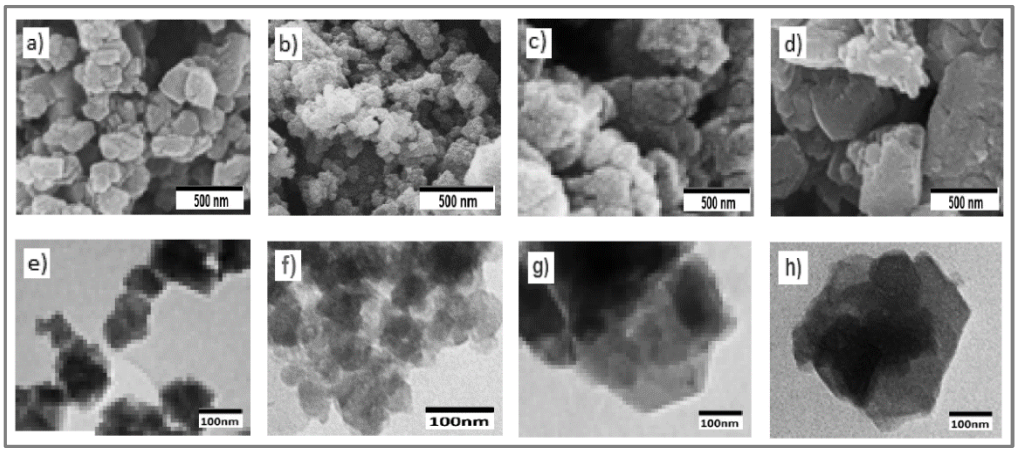

Figure 2. SEM and TEM images of the effects of alkali content on the crystallization of Nano-NaX respectively: NX-3.5N (a) and (e), NX-4.0N (b) and (f), NX -4.5N (c) and (g), NX-5.0N (d) and (h).

Table 2. Effects of alkaline content on nano-NaX crystallization

TT	Sample name	Molar ratio of Na_2O/Al_2O_3 in gel	Crystallinity of zeolite NaX, %	CEC meq $100g^{-1}$	adsorption, % wt		particle size, nm		
					Water	Toluene	XRD	TEM	SEM
1	NX-3.5N	3.5	88	296	26.8	25.9	59	61	85
2	NX-4.0N	4.0	95	320	29.1	27.8	45	45	70
3	NX-4.5N	4.5	91	285	26.3	23.2	56	75	85
4	NX-5.0N	5.0	63+13P1	264	22.1	20.4	74	100+364	120+700

Effects of silicon content: The effects of silicon content on the crystallization of Nano-NaX were investigated by XRD, SEM and TEM methods, presented in figure 3 and figure 4. Table 3 shows the results of crystallinity determination by XRD characterization, the crystal particle size according to XRD, SEM and TEM methods, ion exchange capacity and water, toluene adsorption of the studied samples.

Figure 3 and table 3 shows that, when the molar ratio of SiO_2/Al_2O_3 in the gel increases, the crystallinity of NaX zeolite also increases and reaches a maximum at 95% corresponding to the sample NX-4S with SiO_2/Al_2O_3 ratio = 4.When the ratio of SiO_2/Al_2O_3 continues to increase to 5, there is no peak of NaX zeolite observed, XRD diagram of this sample NX-5S contains only α-quartz and hydroxyl sodalite peak. Thus, when the ratio $SiO_2/Al_2O_3 < 4$, the concentration of SiO_4 tetrahedra

in the gel is low and not enough to link to all AlO_4^- tetrahedra to create Secondary building units (SUB), as a result, the crystallinity is not high.

When the ratio of SiO_2/Al_2O_3> 4, the concentration of SiO_4 tetrahedra in the gel is higher than necessary to combine sufficiently with the AlO_4^- tetrahedra. The excess SiO_4 causes the crystallization process not to produce NaX zeolite but rather to form hydroxyl sodalite with very large and thermodynamically stable crystal (table 3). In figure 4, SEM and TEM images of 4 samples shows that in samples with SiO_2/Al_2O_3 ratio <4, there is still a small amount of amorphous phase which is probably of residual Al_2O_3. The NX-4S sample gives SEM and TEM images with clear, uniform crystals, proving that this sample has high crystallinity, which is consistent with the XRD method determined by 95%.

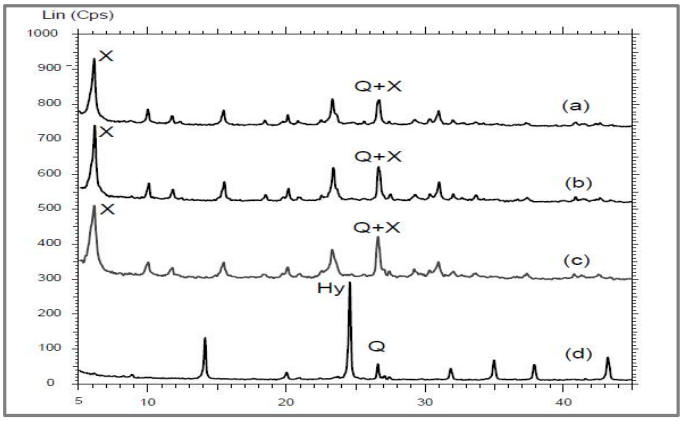

Figure 3. XRD diagram of the effects of silicon content on Nano-NaX crystallization: NX-2S (a), NX-3S (b), NX-4S (c) and NX-5S (d)

Table 3. Effects of silicon content on nano-NaX crystallization

TT	Sample name	Molar ratio of SiO_2/Al_2O_3 in gel	Zeolite NaX crystallinity, %	CEC meq $100g^{-1}$	Adsorption, % wt		Particle size, nm		
					Water	Toluene	XRD	TEM	SEM
1	NX-2S	2	82	273	26.5	24.6	100	100	135
2	NX-3S	3	85	292	27.2	25.1	90	87	110
3	NX-4S	4	95	320	29.1	27.8	45	45	70
4	NX-5S	5	0	15	8.1	3.2	2980	3000	8800

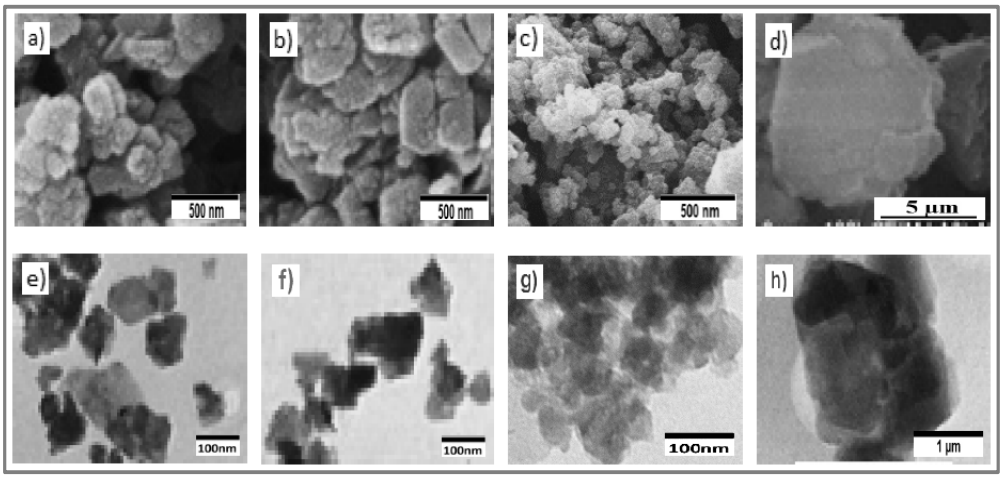

Figure 4. SEM and TEM images of the studied samples on the effects of silicon content on Nano-NaX crystallization: NX-2S (a) and (e), NX-3S (b) and (f), NX-4S (c)) and (g), NX-5S (d) and (h).

In table 3, CEC and absorptivity are linear with crystallinity and particle size of zeolite NaX. NX-4S sample has the smallest particle size in all 3 methods. Crystallinity, CEC, absorptivity of the sample with SiO_2/Al_2O_3 ratio=4 are the highest. Compared with the synthesis of NaX zeolite from different sources, the ratio SiO_2/Al_2O_3= 4 is similar to the results reported in [**22, 24**] from clean chemical, but higher in the report [**9**] when synthesized from rice husk ash and sodium aluminate.

Effects of water: Figure 5, figure 6 and table 4 describe the research results of the effects of water content on the crystallization of Nano-NaX with the application of XRD, SEM, TEM, CEC methods and determine the adsorption of substances which are different in size molecule. When water content is gradually increased, there is no significant change in XRD diagram in figure 5, except that the peaks characteristic of α-quartz have different intensity and the lowest is the sample with molar ratio of H_2O/Al_2O_3=160. With the maximum crystallinity, CEC, the largest adsorption and the smallest, the most uniform particle size, the NX-160H sample is the sample that gave the best results. The XRD and TEM results for crystal size were the same, proving that this very sample is greatly uniform in size. SEM and TEM images are considered to be consistent with the results of phase structure analysis by XRD method, once again, it proves that the molar ratio H_2O/Al_2O_3=160 in the gel system is appropriate for fabricating high crystalline Nano-NaX and small particle size. The molar ratio of H_2O/Al_2O_3 in the sample NX-160H was lower than that reported in [**22, 24**] from clean chemicals, but also higher than in the report [**9**] when synthesized from rice husk ash and sodium aluminate. This difference indicates that, different initial source of material need the different ratio of H_2O/Al_2O_3 in gel system and the crystallization of Nano-NaX always depends on the substances that appear in the gel system at the beginning.

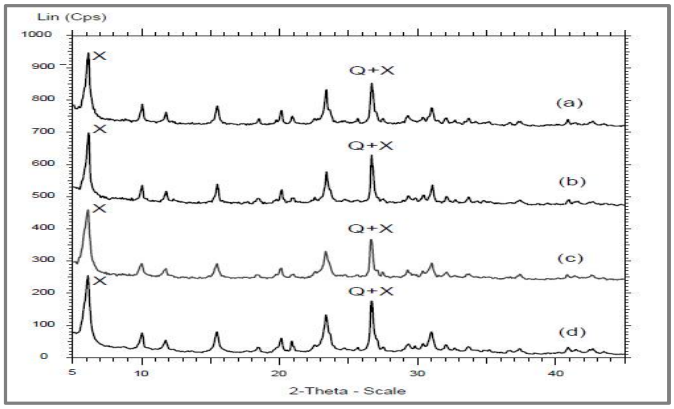

Figure 4. XRD diagram of the effects of water content on Nano-NaX crystallization: NX-140H (a), NX-150H (b), NX-160H (c) and NX-170H (d).

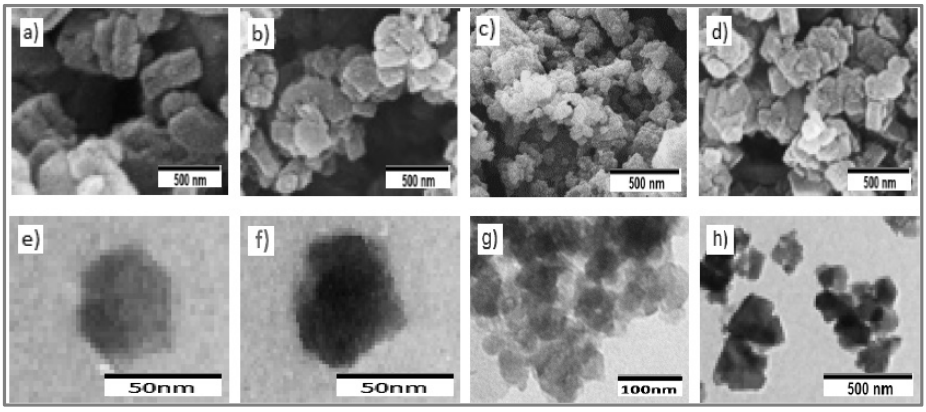

Figure 5. SEM and TEM images of the effects of water content on the crystallization of Nano-NaX: NX-140H (a) and (e), NX-150H (b) and (f), NX-160H, respectively. (c) and (g), NX-170H (d) and (h).

Effect of salt content: The effect of NaCl salt content on the Nano-NaX crystallization process from rice husk ash and calcium carbonate were investigated and presented in figure 7, figure 8 and table 5. From the XRD diagram of the three studied samples in figure 7, it is found that the NX-0NaCl sample without NaCl has a very low ability to crystallize to create Nano-NaX. This sample contains a large amount of amorphous and α-quartz due to XRD diffraction with a high baseline and the α-quartz peak appeared with strong intensity. In the presence of NaCl (samples NX-1NaCl and NX-2NaCl), characteristic peaks of NaX zeolites appeared with a very strong intensity on the XRD diagrams. However, the characteristic peak width of NX-1NaCl is larger, it proves that zeolites NaX crystal particle size in this sample is smaller than in NX-2Cl sample. These results are consistent with TEM, SEM images listed in table 5.

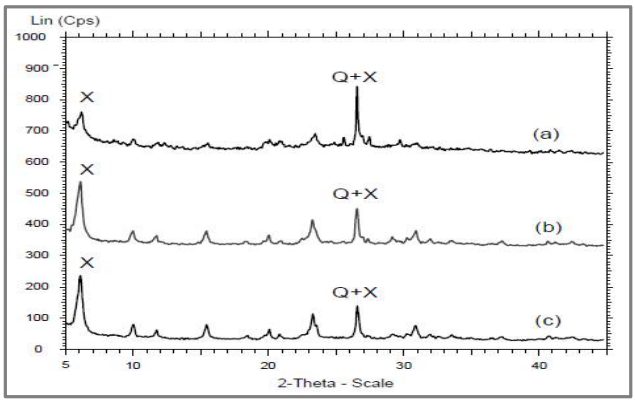

Figure 6. XRD diagram of the effects of salt content on Nano-NaX crystallization: NX-0NaCl (a),NX-1NaCl (b) and NX-2NaCl.

Table 5. Effects of salt content on nano-NaX crystallization

TT	Samples	$NaOH/Al_2O_3$	Crystallinity, %	CEC meq $100g^{-1}$	adsorption, %wt		Partcle size, nm		
					Water	Toluene	XRD	TEM	SEM
1	NX-0NaCl	140	78	256	24.2	23.5	42	44	55
2	NX-1NaCl	150	84	292	26.8	25.5	43	45	68
3	NX-2NaCl	160	95	320	29.1	27.8	45	45	70
4	NX-0NaCl	170	86	285	26.0	25.6	75	146	175

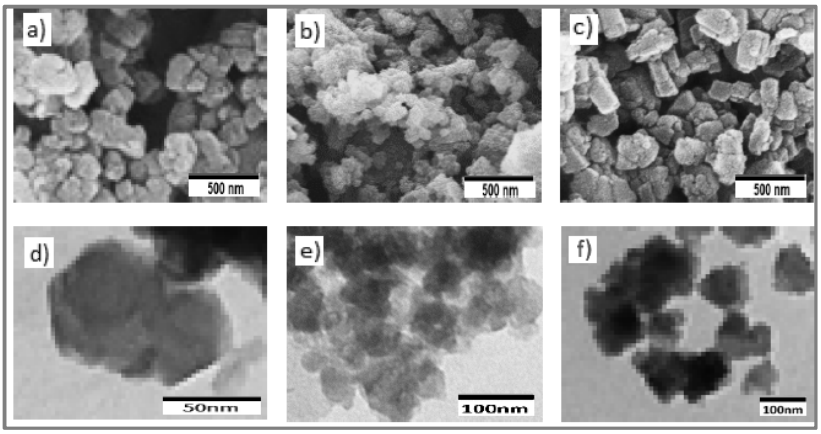

Figure 7. SEM and TEM images of the studied samples on the effects of salt content on the crystallization of Nano-NaX: NX-0NaCl (a) and (d), NX-1NaCl (b) and (e), NX-2NaCl, respectively. (c) and (f).

Thus, the presence of NaCl in the crystallization system increases the ability to combine tetrahedra AlO_4^- and SiO_4 to form germs and at the same time promote the germs to grow into

complete crystals of NaX zeolite. However, the molar ratio $NaCl/Al_2O_3$=1 in the gel is considered to be more optimized than the $NaCl/Al_2O_3$ = 2 ratio due to its higher crystallinity (95 vs. 93%) and especially the more uniform and smaller crystal size (45, 45 and 70 nm compared to 60, 95 and 140 nm with the XRD, TEM and SEM methods respectively used (Table 5).

Effects of aging time: XRD diagram of 3 samples with different aging time is shown in figure 9. Figure 10 shows their SEM and TEM images. Investigation of CDC, absorptivity, crystal particle size in the samples conducted by the methods XRD, TEM and SEM are statistically listed in table 6. Figure 9 shows that characteristic peak of zeolite does not appear in XRD diagram of model NX48-24 (figure 9a) corresponding to aging time of 48 h but only characteristic peak of α-quartz appears at value 2θ ≈. 26.7° with a high amorphous baseline. This result proves the old time of 48 hours is not enough to form zeolite germ. When the aging time increases to 72 h, there are only characteristic peaks of Zeolite NaX appeared at 2θ ≈ 6,2° with high intensity as well as α-quartz peak appeared at 2θ = 26,7° overlapping with a weak peak of NaX zeolite. This sample has a very flat baseline, the characteristic peak width of NaX zeolite is quite large, demonstrating good crystallinity and small size of the crystal particle. Zeolite NaX crystallinity is determined by XRD method and has a value equal to 95%. Scherrer's equation is applied to calculated the average size of NaX crystal which is approximately 45nm. When the aging time increased to 96 h (Figure 9c), XRD diagram show the appearance of characteristic peak of zeolite NaX at 2θ ≈ 6,2°, zeolite NaP1 (P1) at 2θ ≈ 28,1 o and one peak overlapping between α-quartz and NaX zeolite at 2θ ≈ 26.7°. Figure 9c also shows a sharp peak but the baseline is quite high, indicating that the sample contains an amorphous part, NaX and NaP1 zeolite crystals have larger size in sample NX72-24. The XRD method demonstrated that the crystallinity of the zeolites NaX and NaP1 were 42 and 35%, respectively, and the particle sizes were 148 and 659 nm, respectively. Thus, when the aging time increases to 96 hours, the crystallization process is not thorough and selective for NaX zeolite. The simultaneous appearance of two types of zeolite NaX (with 6-sided dual ring structure) and NaP1 (with a single 4-sided ring structure) [**28, 29**] illustrates that the longer the aging process, the more the crystalline germ tends to smaller, and hydrothermal crystallization tends to generate more thermodynamically stable NaP1 zeolite than NaX zeolite [**29**]. Hence, from all the XRD results, the 72 h aging time is the most optimized to create high-crystalline NaX zeolite and small particle size. The presence of weak peaks of α-quartz in the NX72-24 sample is unavoidable because the initial material is from rice husk ash and kaolin. From SEM and TEM images in figure 10, it is found that the sample NX48-24 contains large crystals of α-quartz on an amorphous substrate (Figure 10a), in sample NX72-24 (Figure 10b, 10d), formed crystal has good uniformity and there is no foreign phase appeared except α-quartz. Meanwhile, in sample NX96-24 (Figure 10c, 10e), 2 distinct crystals are observed, small crystals assigned to NaX zeolite and large crystals considered NaP1 zeolites. In the SEM image of this sample, an amorphous part is also observed. All the information and results from table 6 also confirmed that the NX72-24 sample is

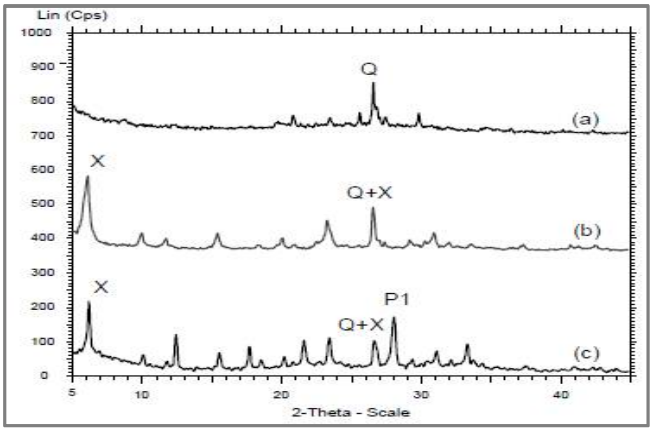

Figure 8. XRD diagram of the studied samples on the effects of aging time on Nano-NaX crystallization: NX-48-24 (a), NX-72-24 (b) and NX-96-24 (c).

well crystallized, the selectivity for the NaX zeolite and the crystal is uniform due to the results measured from XRD and TEM methods equal to 45 nm. The SEM method gives larger size crystals (70 nm) due to its surface reflectance and its lower resolution compared to the transmission and higher resolution of TEM method.

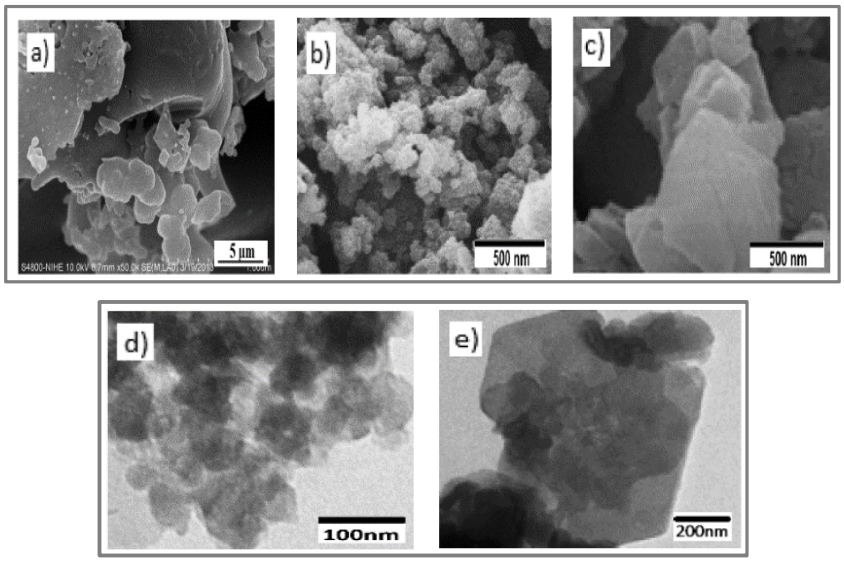

Figure 9. SEM image of sample NX-48-24 (a). SEM and TEM images of samples NX-72-24 (b) and (d), NX-96-24 (c) and (e) respectively.

Table 6. Effects of aging time on nano-NaX crystallization

TT	Sample name	Aging Time	Zzeolite NaX crystallinity, %	CEC meq $100g^{-1}$	Adsorption, % wt		Particle size, nm		
					Water	Toluene	XRD	TEM	SEM
1	NX-48-24	48	0	56	5,4	4,6	-	-	Q+Amorphous
2	NX-72-24	72	95	320	29,1	27,8	45	45	70
3	NX-96-24	96	42X+35P1	216	20,3	16,4	148+65 9	155+860	260+930+ Amorphous

In table 7, the results of CEC determination and the adsorption of 3 samples also showed that the sample NX72-24 had the highest CEC and the highest adsorption capacity. In particular, CEC=320 meq 100 g^{-1} shows that this sample contains a large portion of AlO_4^- tetrahedra. CEC of the sample containing zeolite NaX is such high only because this sample has very high crystallinity. This conclusion is consistent with all results obtained from the XRD, SEM and TEM methods discussed above.

Influence of crystallization time: If the aging stage produces seed crystal from different types of coupling between the $AlO_4^-$and SiO_4 tetrahedra, the crystallization stage is considered to be the process promoting the growth of crystal sprouts. That helps form the complete crystals of zeolites. From the XRD diagram of crystalline samples with the time of 12, 24 and 36 h in figure 11, it was shown: When the crystallization time of the typical peak in zeolite NaX increases and reaches its maximum in the sample NX72-24, it corresponds to the 24-h crystallization time. When the crystallization time increased to 36 h, zeolite NaP1 appeared with an amorphous baseline. This proves that short crystallization time (12 h) is not enough for the seed crystal to grow into crystals. But when the crystallization time is long (36 h), a part of NaX zeolite crystal (created after 24 h of crystallization) will change phase into zeolite NaP1 and the amorphous baseline reappeared due to the AlO_4^- tetrahedron transformed into amorphous Al_2O_3 (Because NaX and NaP1 zeolites have SiO_2/Al_2O_3 ratio respectively 2.5 and 3.3).

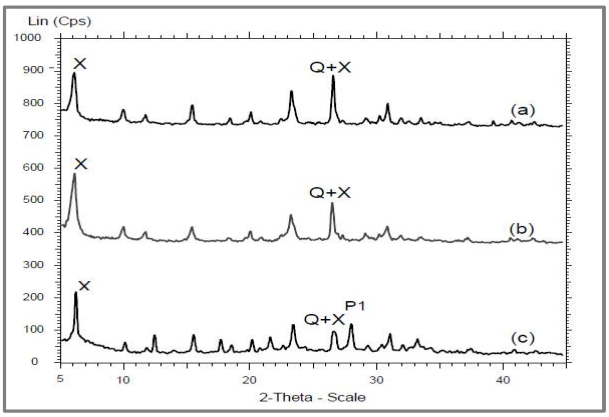

Figure 11. XRD patterns of samplesaffecting the crystallization time: NX-72-12 (a), NX-72-24 (b) và NX-72-36 (c).

Table 7. The influence of crystallization time on Nano-NaX

S.No	Samples	Time of crystallization	Crystallinity zeolite NaX, %	CEC meq $100g^{-1}$	Adsorption, % weight		Crystal particle size, nm		
					Water	Toluene	XRD	TEM	SEM
1	NX-72-12	12	85	283	25,4	25,0	42	105	125+VĐH
2	NX-72-24	24	95	320	29,1	27,8	45	45	70
3	NX-72-36	36	58X+23P1	275	21,5	18,2	50+358	50+435	70+890+VĐH

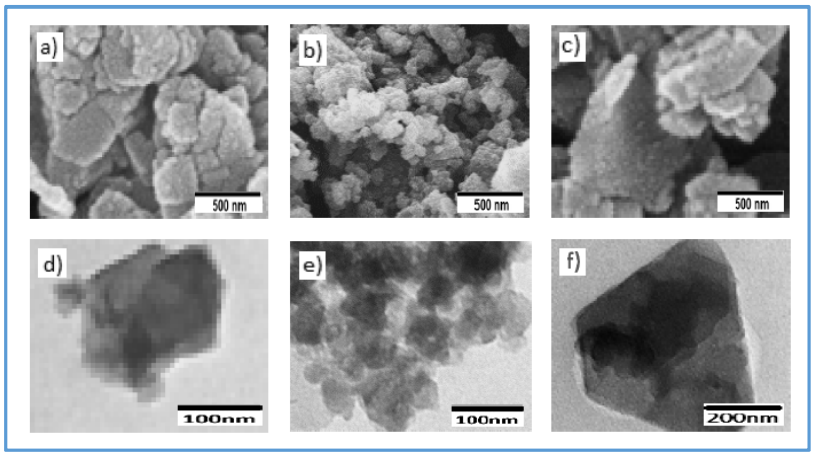

Figure 12. SEM and TEM images of the research samples influence the crystallization time on the Crystallization Nano-NaX: NX-72-12 (a) and (d), NX-72-24 (b) và (e), NX-72-36 (c) và (f).

NaX zeolite crystals were determined corresponding to 12, 24 and 36 h crystallization time by 85, 95 and 58%. In the NX72-36 sample, there are 23% zeolite NaP1 remaining. From figure 12 and table 7, the results of determination of particle size according to XRD, TEM, SEM methods showed that only NX72-24 samples appeared crystal uniformly. The other two samples are less uniform crystals and contain an amorphous baseline. The low toluene adsorption in the NX72-36 sample is due to NaP1 zeolite having a capillary size smaller than toluene molecular diameter [**28, 29**]. Thus, under the stated experimental conditions, a 24 h crystallization time is appropriate to create Nano-NaX crystals.

Influence of crystallization temperature: The crystalline temperature is an important parameter that contributes to speeding up the formation of crystals from seed crystal formed during aging. However, they also affect the size of the crystal formed.

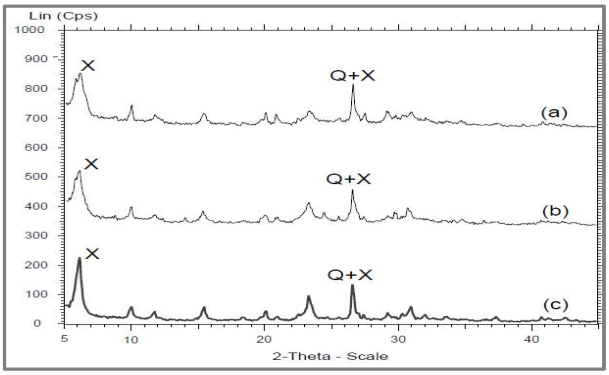

Figure 13. XRD patterns of samples affecting the temperature of crystallization on crystallization Nano-NaX: NX-75^{0}C (a), NX-85^{0}C (b) and NX-95^{0}C (c).

In figure 13, the XRD diagram of crystallized samples at different temperatures showed significant differences. When increasing the crystallization temperature, the amorphous phase gradually transformed into crystalline phase zeolite Nax,the peak characteristic for NaX zeolite has increasing intensity along with the decreasing peak width. This means that, when the crystallization temperature increases, the crystallinity of NaX zeolite increases with increasing particle size, similar to the crystallization of Nano-NaX from clean chemicals [23].

Table 8. The Influence of crystallization temperature on the crystallization Nano-NaX

No	Samples	Crystallization temperature, °C	Crystallinity zeolite NaX, %	CEC meq 100 g^{-1}	Adsorption, % Weight		Crystal particle size, nm		
					Water	Toluene	XRD	TEM	SEM
1	NX-75 °C	75	80	220	23,5	22,1	32	43	50+VĐH
2	NX-85 °C	85	82	265	25,2	25,4	38	45	60+VĐH
3	NX-95 °C	95	95	320	29,1	27,8	45	45	70

The results in table 8 corresponding to the samples NX-75°C, NX-85°C and NX-95°C (NX-72-24), the crystal and size of NaX zeolite particles were determined by 80 % and 32 nm, 82 % and 38 nm, 95 % and 45 nm. The results of TEM and SEM capture in figure 14 and the measurement of particle size statistics in Table 8 showed a very good correlation with the XRD results. CEC capacity and adsorption are consistent with the determination of crystal size and particle size zeolite. It is noteworthy that all three samples are appearing peaks of α-quartz weak. This is inert SiO_2 that is not metabolized from the starting material. Therefore, it can be assumed that Nano-NaX = 95 % crystallinity in the samples NX-95°C is the desired value, so do not need to survey at higher temperatures because it will consume more energy, especially when done above 100°C will arise difficulties due to increased pressure of the crystallization process.

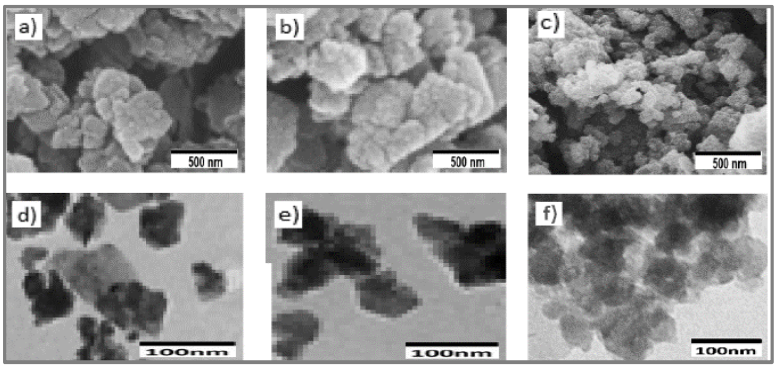

Figure 14. SEM and TEM images of the research samples influence the crystallinity temperature on the crystallization Nano-NaX: NX-75 ^{0}C (a) and (d), NX-85 ^{0}C (b) and (e), NX-95 ^{0}C (c) and (f).

Nano-NaX characteristics are synthesized under appropriate conditions: The XRD diagram of the Nano-NaX sample in this researchand the Nano-NaX sample comparing the synthesis of pure chemicals by microwave method [23] is shown in figure 14. From this it is found that these two XRD diagrams have a good correlation because the X-ray diffraction at their2θ values coincides with the NaX zeolite which is the international crystal PDF 38-0237, the formula $Na_2O{\cdot}Al_2O_3{\cdot}2.5SiO_2{\cdot}6.2H_2O$. It is noteworthy that It is worth noting that the peak width of the peak, especially at the NaX zeolite peak at 2θ ≈ 6, 20, is very large, proving that these samples have very small particle size.

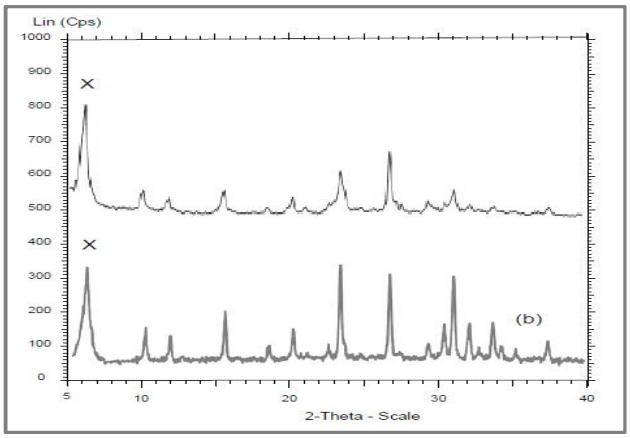

Figure 14. XRD patterns of samples nano-NaX synthesized (a) and Nano-NaX according to [23] (b).

The appearance of NaX zeolite peaks with strong intensity and almost no strange phase confirms that these samples have very high crystallinity. If [23] is synthesized by the microwave method at a temperature of 90°C for 3 h from pure chemicals, giving a Nano-NaX crystal equal to 99 %, the Nano-NaX crystal in this study is determined. determined by XRD method by 95%. We know that rice husk ash and Metakaolin are not clean chemicals, so the small amount of impurities that follow the product is inevitable.

Figure 15 presenting SEM and TEM of the Nano-NaX sample from this research (figure 15a, 15d) compared with the SEM image of Nano-NaX synthesized from pure chemicals by the hydrothermal method [22] (figure 15b) and microwave method [24] (figure 15c). Table 2 shows the synthesis conditions and characteristics of Nano-NaX from different methods to verify. Figure 15, SEM image

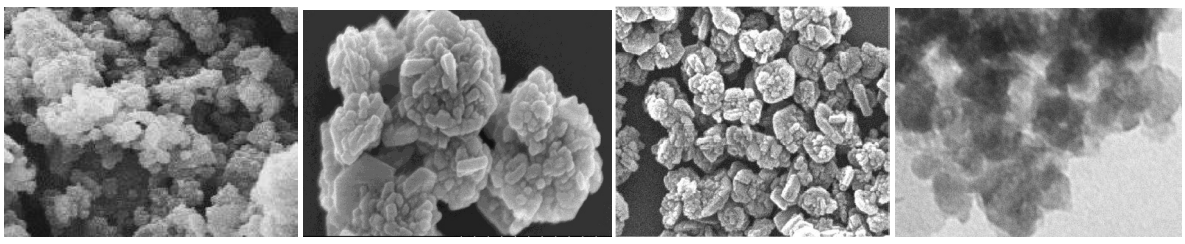

Figure 15. SEM images of the samples nano-NaX synthesized (a) and nano-NaX according to [22] (b), Nano-NaX according to [24] (c). TEM image of the sample nano-NaX synthesized (d).

observation of three samples (Figure 15a, 15b, and 15c) has noted that they are located in the nanoscale size and fairly uniform, barely seen strange phase. The SEM method also showed the clumping of many small particles due to the nano effect, and the average particle size was determined by 70, 20-100 and 70 nm, respectively. Figure 15d shows a TEM image of the Nano-NaX sample in this report, with an average crystal size of 45 nm. The difference in measurement results between SEM and TEM methods when determining particle size is due to the difference in the nature of each method as well as the resolution of the lower SEM method compared to the TEM method. The

uniformity of particle size (45 nm) when determined by XRD and SEM methods showed that the sample Nano-NaX synthesized was small and very uniform, unlike the results obtained from the project [22] (Table 9).

FTIR spectrum of Nano-NaX sample synthesized and comparison sample from the project [22] is presented in figure 16. It can be seen that all spectral clusters appearing in the survey ranged from 400-1300 cm^{-1} are like each other, with not much different intensity. The peak characterizes the hexagonal double-ring oscillation in the micro-sized NaX zeolite only at 566 cm^{-1} appeared with other spectral clusters at 607-608 cm^{-1}, which only appeared when NaX zeolite was nano-sized [24]. In addition, the presence of spectral cluster 680-681 cm^{-1} was assigned to the oscillation of sinanol (Si-OH) bonding with silicon in the Q3 [31] form. This spectral cluster appears only in the nanoscale FAU zeolite structure [22], but not in the structure Q4 of the micro-sized FAU zeolite [31, 32].

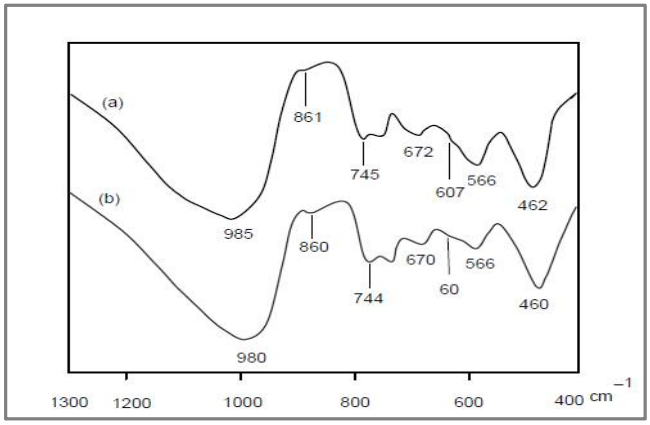

Figure 16. The IR spectrum of the samples nano-NaX synthesized (a) and nano-NaX according to [22] (b)

N_2 adsorption-desorption isotherms and the pore distribution of the nano-NaX synthesized and comparison samples from the report [22] are shown in figure 17. Both of these schemes appear to delay loop starting at P/Po ≈ 0.55 characterizing form III according to IUPAC classification [1.33] due to condensation of N_2 in the mesoporous materials. With Nano-NaX materials, mesoporous materials can only be formed from the intergranular gap due to the clustering of nanoscale crystals, similar to those discussed in [22, 24]. The individual surface areas measured are 492 and 530 $m^2 g^{-1}$, respectively. This difference is probably due to the larger Nano-NaX crystal size in the synthetic sample than in the comparison sample (45 vs. 23 nm, respectively-according to the XRD method, table 9). The pore distribution of the synthetic sample (Figure 17A), in addition to the micro-capillary concentration at 0.8 nm similar to the comparison sample (Figure 17B), mesoporous materials concentration at 5.5 nm is narrower than that of 9, 8 nm in the verify sample.

Table 9. CEC, adsorption and crystal size of the research samples

No	Samples	Method	Temperature °C	Time, hour	Crystallinity, %	specific surface, $m^2 g^{-1}$	CEC Meq $100g^{-1}$	Particle size, nm		
								XRD	TEM	SEM
1	Nano-NaX synthesized	Hydrothermal	95	24	95	492	320	45	45	70
2	Nano NaX according to [28]	Hydrothermal	60	48	99	530	-	23	-	20-100
3	Nano NaX according to [27]	microwave	90	3	100	536	-	-	-	70

TEOS: tetraethyl orthosilicate (aldrich); SM-30: SM-30 colloidal silica (aldrich); Fumed silica (aldrich).

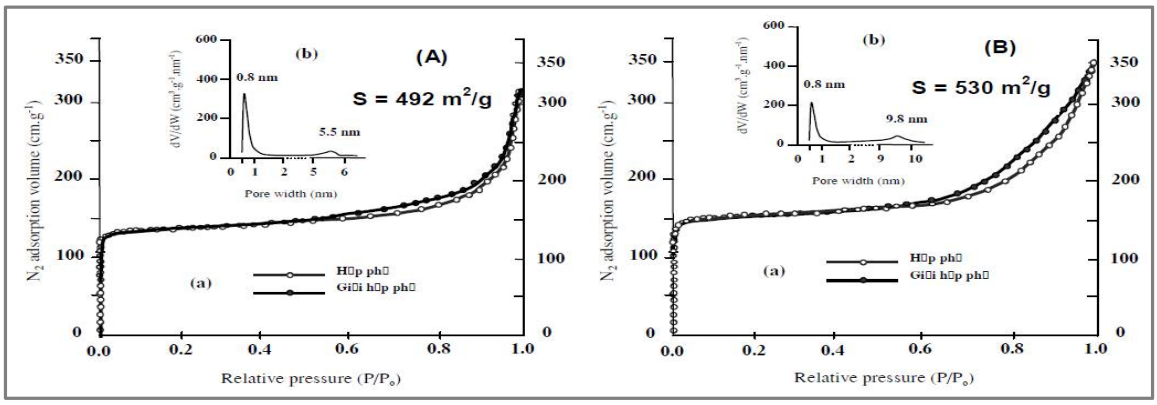

Figure 17. The Adsorption-desorption isotherms N_2 (a) and the pore-size distribution (b) on the sample nano-NaX synthesized (A) and nano-NaX according to [22] (B).

According to the report [9], the micro-sized NaX zeolite synthesized from rice husk ash and sodium aluminate with CEC determined by NH_4^+ equal to 317 meq NH_4^+ 100 g^{-1} and the specific surface BET is 676 m^2 g^{-1}. Although the Nano-NaX sample synthesized in this project only has a BET area of 492 m^2 g^{-1}, the CEC is determined by 320 meq Ba^{2+} 100 g^{-1} (equivalent to 640 meq NH_4^+ 100 g^{-1}). This proves that CEC strongly depends on particle size, in other words, the larger CEC, the smaller the particle size, and when the particle size is smaller, the larger the outer surface area will quickly increase the ion exchange and adsorption capacity. This is also the preeminent property of the nanoscale zeolite material compared to the micro-sized conventional zeolite.

Nano-NaX application in poor quality diesel fuel treatment:

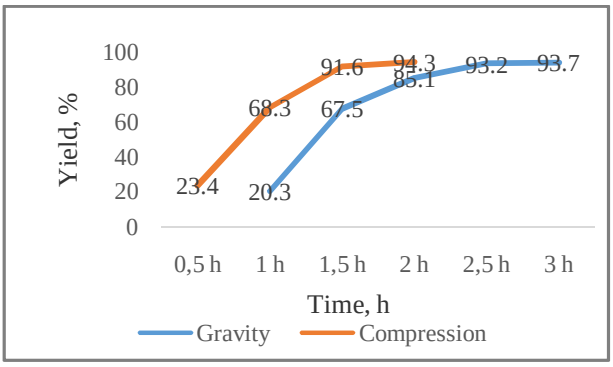

Figure 18. The influence of time on poor quality diesel adsorption efficiency.

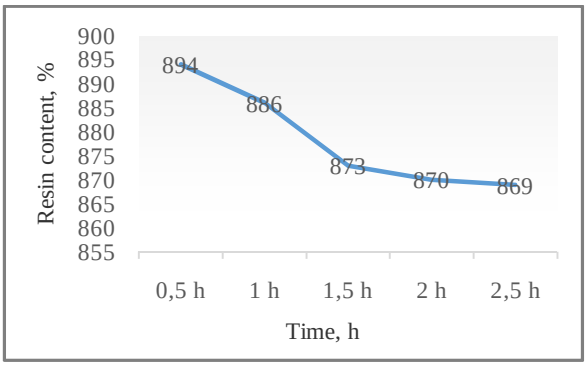

Figure 19. Influence of mixing process in the gum content to fuel contamination.

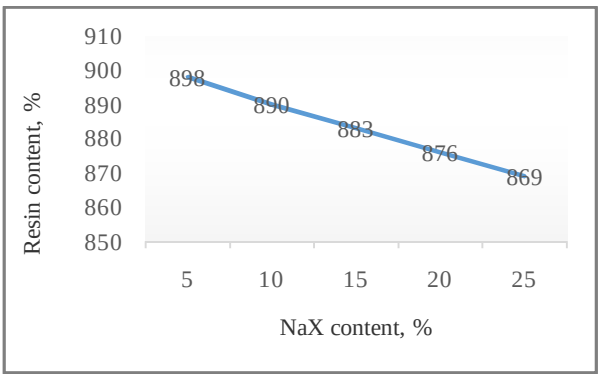

Figure 20. Influence of NaX content on the gum content in contaminated fuel

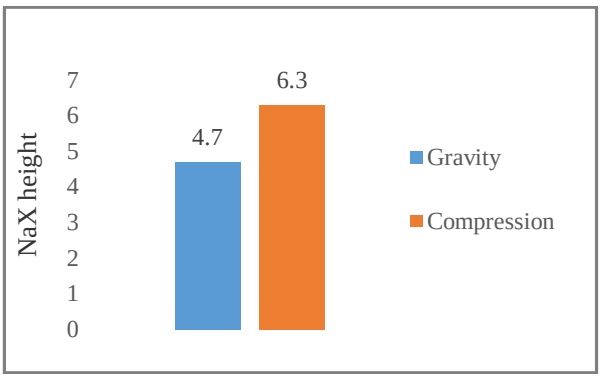

Figure 21. Influence of compressive force on the height of NaX zeolite adsorption.

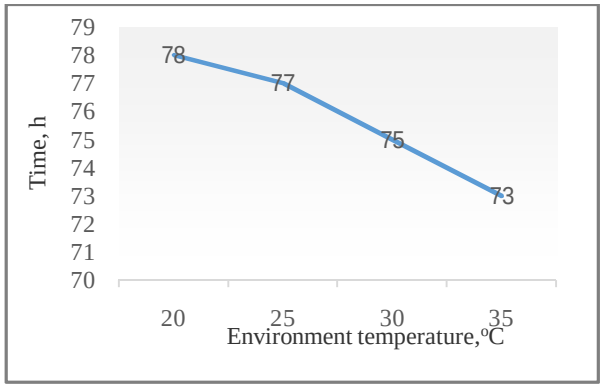

Figure 22. Influence of temperature on poor quality diesel treatment time

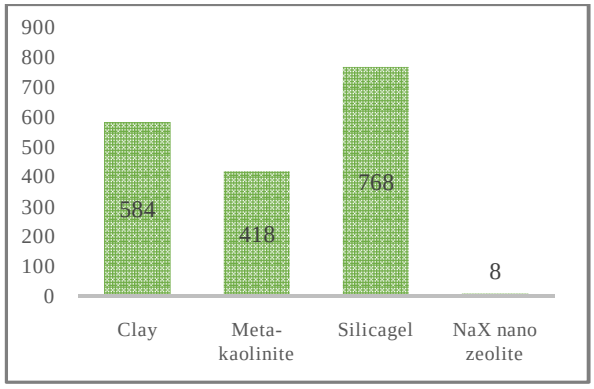

Figure 23. Influence of the adsorption on poor quality diesel treatment.

From the above results, we can see that the gum content in the fuel treated lowest when using nano NaX zeolite.This content has met the current standards of diesel fuel. The remaining adsorbents have reduced the amount of gum in the fuel, but there are still many colors of the fuel that are still black; The fuel after treatment has a high gum content, unsatisfactory quality.

APPLICATION

Nano NaX zeolite synthesized from rice husk and kaolin was used to treat the polluted diesel fuel by adsorption method. The process provided an effective solution for reusing or screening the waste diesel fuels.

CONCLUSION

Researching the factors that influenced the formation of nano-Nax. Accordingly, all investigated factors have influence on the formation of nano-NaX. Proposed a new method to synthesize new Nano-NaX directly from rice husk ash and Metakaolin under hydrothermal conditions at 95°C for 24 h. The obtained product has a crystallinity of 95%, particle size 45 nm, exchange capacity 320 meq Ba_2^+/100g, specific surface BET 492 m^2 g^{-1}, pore distribution is concentrated in the microcapillary area 0, 8 nm and capillary averaging 5.5 nm. Researching the factors that influenced the adsorption of poor-quality diesel fuel treatment. Accordingly, all investigated factors have influence on the adsorption of diesel fuel treatment. Proposed the process of treating poor quality diesel fuel by adsorption treatment via nano NaX zeolite at ambient temperature conditions.

REFERENCES

[1]. Tangoc don, Vatlieumaoquantu cao lanh Vietnam: Tong hop, dac trung va ung dung NXB bachkhoa-Ha noi, 2012. ISBN 9786049112430.

[2]. K. Shams, S. J. Mirmohammadi, Preparation of 5A zeolite monolith granular extrudates using kaolin: Investigation of the effect of binder on sieving/adsorption properties using a mixture of linear and branched paraffin hydrocarbons, *Microporous and Mesoporous Materials*, **2007**, 106, 268–277.

[3]. Doaa M. EL-Mekkawi, Mohamed M. Selim, Removal of Pb^{2+} from water by using Na-Y zeolites prepared from Egyptian kaolins collected from different sources, *Journal of Environmental Chemical Engineering*, **2014**, 2(1), 723-730.

[4]. Ian D.R. Mackinnon, Graeme J. Millar, Wanda Stolz, Hydrothermal syntheses of zeolite N from kaolin, *Applied Clay Science*, **2012**, 58, 1-7.

[5]. Ebrahim Mohiuddin, Yusuf Makarfi. Isa, Masikana M. Mdleleni, NonyamekoSincadu, David Key, Themba Tshabalala, Synthesis of ZSM-5 from impure and beneficiated Grahamstown kaolin: Effect of kaolinite content, crystallisation temperatures and time, *Applied Clay Science*, **2016**, 119, 213–221.
[6]. Ebrahim Mohiuddin, Yusuf Makarfi Isa, Masikana M. Mdleleni, David Key, Effect of kaolin chemical reactivity on the formation of ZSM-5 and its physicochemical properties, *Microporous and Mesoporous Materials*, 2017, 237, 1-11.
[7]. AijunDuan, Guofu Wan, Ying Zhang, Zhen Zhao, Guiyuan Jiang, Jian Liu, Optimal synthesis of micro/mesoporous beta zeolite from kaolin clay and catalytic performance for hydrodesulfurization of diesel, *Catalysis Today*, **2011**, 175, 485-493.
[8]. Diego Ivan Petkowicz, Reus Tiago Rigo, Cláudio Radtke, Sibele B. Pergher, Jo. o H.Z. dos Santos, Zeolite NaA from Brazilian chrysotile and rice husk, *Microporous and Mesoporous Materials*, **2008**, 116, 548–554.
[9]. Hiroaki Katsuki, Sridhar Komarneni, Synthesis of Na-A and/or Na-X zeolite/porous carbon composites from carbonized rice husk, *Journal of Solid State Chemistry*, **2009**, 182, 1749-1753.
[10]. A. M. Yusof, N. A. Nizam, N. A. A. Rashid, Hydrothermal conversion of rice husk ash to faujasite-types and NaA-type of zeolites, *J. Porous Mater*., **2010**, 17, 39-47.
[11]. L. T. H. Nam, T. Q. Vinh, N. T. T. Loan, L. K. Lan, L. Q. Du, Microwave hydrothermal synthesis of hierachical porous solid acid ZSM-5/SBA-15 (MAS-9); ZSM-5/SBA-16 using silica source from vietnam rice husk (RH) and catalytic performance for etherification of limonene, *Journal of Chemistry* **2009**, 47(6A), 567-571.
[12]. T.Q. Vinh, N.T.T. Loan, L.T.H. Nam, C.V. Giáp, Tạp chí Hóa học, **2009**, 47(6B), 103-109.
[13]. P. Khemthong, S. Prayoonpokarach and J. Wittayakun, Suranaree, Synthesis and characterization of zeolite LSX from rice husk silica, *J. Sci. Technol*., **2007**, 14(4) 367-379.
[14]. R.M. Mohamed, I.A. Mkhalid, M.A. Barakat, Rice husk ash as a renewable source for the production of zeolite NaY and its characterization, *Arabian Journal of Chemistry*, 2015, 8,48-53.
[15]. M. K. Naskar, D. Kundu, M. Chatterjee, Synthesis of ZSM-5 Zeolite Particles Using Triethanol Amine as Structure-Directing Agent, *J. Am. Ceram. Soc*., **2012**, 95, 925.
[16]. Kartick P. Dey, Sourav Ghosh, Milan K. Naskar, A facile synthesis of ZSM-11 zeolite particles using rice husk ash as silica source, *Materials Letters*, **2012**, 87, 87–89.
[17]. A. Y. Atta, B. Y. Jibril, B. O. Aderemi, S. S. Adefila, Preparation of analcime from local kaolin and rice husk ash, *Applied Clay Science*, **2012**, 61, 8–13.
[18]. TaNgo don, Le Vanduong, TaNoc Hung, Ta Nogoc Thien Huy Nguyen Thi Xuan, Nguyen huru Duc, nguyen DucNghia NinhThiPhuon, Chuyenhoathuyanhiettrotrauvameta caolanh thanhmsozeolitNay, TachiXuctacvaHapphu, **2014**, 3(3), 59-63.
[19]. TaNgocDon, TrinhXuanBai, Le Van Duong, Ta Ngoc Hung, Nguyen Manh Cuong,Tran VanHuong, NguyenHuuDuc, Nghiencuutonghopvatlieu MSU-S(Y) tutrotrauvametacaolanh, Tapachixuctacva Hap phu, **2015**, 4(3), 131-137.
[20]. Jing-Quan Wang, Ya-Xi Huang, Yuanming Pan, Jin-Xiao Mi, New hydrothermal route for the synthesis of high purity nanoparticles of zeolite Y from kaolin and quartz, *Microporous and Mesoporous Materials*, **2016**, 232, 77–85.
[21]. Marcos Antonio Klunk, Suellen BrasilSchröpfer, Sudipta Dasgupta, Mohuli Das, Nattan Roberto Caetano, Andrea Natale Impiombato, Paulo Roberto Wander & Carlos Alberto Mendes Moraes, Synthesis and characterization of mordenite zeolite from metakaolin and rice husk ash as a source of aluminium and silicon, *Chemical Papers*, **2020**, 74 (), 2481–2489.
[22]. Bi-Zeng Zhan, Mary Anne White, Michael Lumsden, Jason Mueller-Neuhaus, Katherine N. Robertson, T. Stanley Cameron and Michael Gharghouri, Control of Particle Size and Surface Properties of Crystals of NaX Zeolite, *Chem. Mater*., **2002**, 14(9), 3636–3642.
[23]. Mahdi Ansari, AbdolrezaAroujalian, AhmadrezaRaisi, Bahram Dabir, Mahdi Fathizadeh, Preparation and characterization of nano-NaX zeolite by microwave assisted hydrothermal method, *Advanced Powder Technology*, **2014**, 25, 722–727.

[24]. HàThị Lan Anh, Nghiêncứutổnghợp nano-zeolit NaX từcaolanhViệt Nam cósửdụngphụgiahữuco, Luậnántiếnsĩ, HàNội , **2012**.
[25]. J. Dewis, F. Freitas, Physical and chemical methods of soil and water analysis, FAO soils Bulletin, **1984**, 10, 106.
[26]. A. Petushkov, J. Freeman, S.C. Larsen, Framework Stability of Nanocrystalline NaY in Aqueous Solution at Varying pH, *Langmuir*, **2010**, 26(9), 6695–6701.
[27]. H. Yin, T. Zhou, Y. Liu, Y. Chai, C. Liu, Synthesis of high-quality nanocrystalline zeolite Y using pseudoboehmite as aluminum source, Journal of Porous Materials, **2012**, 19(3), 277-281.
[28]. D. W. Breck, Zeolite Molecular Sieves, Wiley, New York, **1974**.
[29]. Hong K.D. Nguyen, Don N. Ta and Hung N. Ta, Effects of Synthetic Conditions on Structure of Nanocrystal Zeolite Y from Vietnamese Kaolin, *J.Applicable Chem.*, **2017**, 6(1) 50-68.
[30]. Mansoor Kazemimoghadam, TorajMohammadi, Preparation of nano pore hydroxysodalite zeolite membranes using of kaolin clay and chemical sources, Desalination **2011**, 278, 438-442.
[31]. J. Klinowski, Solid-state NMR studies of molecular sieve catalysts, *Chem. Rev.*, **1991**, 91, 1459.
[32]. C. A. Fyfe, G. T. Kokotailo, NATO ASI Ser. C: *Math. Phys. Sci.*, **1994**, 447, 277.
[33]. M. Kruk, M. J aroniec, Gas Adsorption Characterization of Ordered Organic−Inorganic Nanocomposite Materials, *Chem. Mater.*, **2001**, 13, 3169.